Supplemental Information

Materials

Antibodies for RIP3 were purchased from ABGENT, San Diego, CA; pSer^{345} MLKL (ab196436) and MLKL (ab172868) from Abcam, Cambridge, MA; TNFα (#70R-TR008) from Fitzgerald Industries International, Acton, MA; collagen 1 from Southern Biotech (Birmingham, AL); HSC70 and IRS-1 (sc-8038) from Santa Cruz Biotechnology (sc-7298), Dallas, TX; caspase-3 (#9665), PARP (#9544) and beta-actin(#4967) from Cell Signaling, Danvers, MA and pSer^{307}IRS-1(44-813G) from Thermo Fisher Scientific, Grand Island, NY. Custom antibodies against 4-HNE modified proteins were from Alpha Diagnostics, San Antonio, TX. TUNEL assay kit (Apop Tag @ Plus in Situ apoptosis detection kit) was purchased from Millipore (Billerica, MA cat. no. S7111). Caspase-generated fragments of cytokeratin-18 were detected using M30 staining kit (Roche, Mannheim, Germany). MLKL-/- mice were from Taconic, Hudson, NY. MTS cytotoxicity kit CellTiter 96 AQueous One Solution Cell Proliferation Assay (Promega, Madison, WI; Cat# G3581). AML12 cells were from ATCC (Manassas, VA; cat#:CRL-2254). Cell culture media were from Sigma Aldrich (St. Louis, MO) and medium supplements were from Gibco ThermoFisher (Grand Island, NY) and Cayman Chemicals (Ann Arbor, MI). Propidium Iodide assays for live cell imaging were from Life Technologies (Eugene, OR).

Methods

Mouse handling and tissue collection

Animals were housed in pairs in standard microisolator cages and maintained on a 12 h:12 h light/dark cycle. At the end of the HFD feeding protocol, mice were fasted for 6 hours prior to euthanasia. Mice were weighed weekly and food intake per cage measured weekly. Portions of

liver and epididymal adipose tissue were flash frozen in liquid nitrogen and stored at -80^{o}C, preserved in RNAlater (Ambion/Life Technologies) and stored at -20°C until RNA isolation, or fixed in 10% formalin or frozen in optimal cutting temperature (OCT) compound (Sakura Finetek U.S.A., Inc., Torrance, CA) for histology. Blood was transferred to EDTA-containing tubes for the isolation of plasma. Plasma was then stored at -80°C.

Energy Expenditure

To measure energy expenditure, mice were fed the HFD or chow diets for 9 weeks and then transferred to the Columbus Instruments Comprehensive Lab Animal Monitoring System (Oxymax/CLAMS, Columbus Instruments, Inc). Food and water intake, VO_2 and VCO_2 were measured every 10 min for 168 h (1 wk). Respiratory exchange rate was calculated from VO_2 and VCO_2. Subsequently, the mice were transferred to standard housing and were continued on the HFD or chow diets until they were used for glucose tolerance tests.

To account for body size variation on total energy expenditure (1), group comparisons involving this outcome were adjusted for total body mass using multiple-regression analysis as recommended by Kaiyala and colleagues (2, 3). The analysis of covariance (ANCOVA) was performed using the linear mixed model procedure (http://www.mmpc.org/shared/regression.aspx). Analyses were done within the photoperiod and encompassed four light and four dark cycles as repeated measures with a compound symmetry covariance structure. Differences were considered significant when $P < 0.05$, 2-tailed.

Glucose tolerance tests. Fasting blood glucose was measured from a tail nick using the OneTouch Ultra Blood Glucose Meter and test strips (Lifescan, Milpitas, CA). Glucose tolerance tests were performed on 6-h fasted mice after 14 weeks of high-fat diet feeding. For glucose tolerance tests, mice received 25% D-glucose solution (2 mg/kg of bodyweight) or an equal volume of saline by intraperitoneal injection; blood glucose was measured at baseline, 15, 30, 60, and 120 minutes. Fasting insulin was measured in plasma samples using a commercially available ELISA kit (Mercodia, Uppsala, Sweden). HOMA-IR was calculated using the following formula: (fasting glucose (mg/dl) x fasting insulin (ng/ml))/405.

Biochemical assays

Plasma samples were assayed for alanine aminotransferase (ALT) and aspartate aminotransferase (AST) using commercially available enzymatic assay kits (Sekisui America Corp, Seacacus, NJ) following the manufacturer's instructions. Total hepatic triglycerides were assayed using the Triglyceride Reagent Kit from Pointe Scientific Inc. (Lincoln Park, MI). Plasma cholesterol, beta-hydroxybutyrate, non-esterified fatty acids and triglycerides were measured by Marshfield Laboratories (Marshfield, WI).

Isolation of RNA and quantitative real-time polymerase chain reaction (qRT-PCR)

Total RNA was isolated from liver tissue and reverse transcribed followed by amplification using qRT-PCR. 25 µl of reaction mix contained cDNA, Power Syber Buffer (Applied Biosci/Life Technologies) and primers at final concentrations of 10 µM. qRT-PCR was performed in the Mx3000P cycles of 15 s at 95 ^{o}C, 30 s at 60 ^{o}C, 30 s at 72 ^{o}C followed by 1 min at 95 ^{o}C, 30 s at 55 ^{o}C and 30 s at 95 ^{o}C. The relative amount of target mRNA was determined

using the comparative threshold (Ct) method by normalizing target mRNA Ct values to those of 18S (4). Primer sequences are listed in Supplemental Table 2.

PCR Array Analysis

Total RNA was isolated from mouse liver using the RNeasy micro kit (Qiagen, USA) according to the manufacturer's instruction. Concentration and purity of isolated RNA were measured using the NanoDrop1000 spectrometer and samples were screened for an A260 : A280 ratio greater than 1.8. Conversion of RNA to cDNA was carried out using 50 ng of RNA according to the manufacturer's instructions for the RT^2 First Strand Synthesis Kit (Qiagen, USA). Samples were prepared from pooled RNA extracted from livers from 3 chow and 3 HFD mice.

The mouse insulin resistance (PAMM-156Z) focused pathway array (RT^2 Profiler^{TM} PCR Array Mouse Insulin Resistance, Qiagen) in a 96 well plate format was use to assess changes in hepatic gene expression. The cDNA from individual samples was added to the reaction plates following the manufacturer's instructions using SYBR green and array analysis was performed using the Strata Gene Mx3000p system. Quality control tests for genomic DNA control, reverse transcription control and positive PCR control were included in each array plate. Data were analyzed using SABiosciences RT2 Profiler PCR Data Analysis software (available at http://pcrdataanalysis.sabiosciences.com/mirna/arrayanalysis.php) and were considered significant at >2.0-fold change. Three housekeeping genes not influenced by the experimental condition (*Hsp90ab1, Gapdh* and *Actb*) were used for normalization. Fold changes for each detectable gene are shown in Supplemental Table 1.

Western blot analysis

Frozen liver was homogenized in lysis buffer (~50 mg tissue/ml). Protein concentrations were measured in lysates from liver and AML12 hepatocytes with the DC protein assay kit from Bio-Rad (Hercules, CA). Proteins were separated by SDS-PAGE for Western blot analysis. HSC70 was used as a loading control.Western blot analysis was performed using enhanced chemiluminescence for signal detection. Signal intensities were quantified by densitometry using Image J software (NIH, Bethesda, MD).

Culture and transfection of AML12 cells

AML12 cells were cultured in DMEM/F12 with 10% FBS, supplemented with insulin, transferrin, selenium and dexamethasone, as per ATCC instructions. In some experiments, cells were pretreated with the pan-caspase inhibitor Z-VAD, necrostatin-1 (an inhibitor of RIP1 kinase), CA-074 (an inhibitor of cathepsin-B) or actinomycin D. In other experiments, in order to knock-down RIP3, cells were subcultured in 24-well plates at 0.044 x 10^6/ml/well or 96-well plates at 0.007 x 10^6/200ul/well. After 6 hrs, cells were transfected with scrambled siRNA or siRNA targeted against RIP3 (ON-TARGETplus SMARTpool siRNA cat# L-049919-00-0005; Target sequence: UCAAGAUCGUGAACUCGAA, CAAGUUCGGCCAAGUAUGA, GGUAAAGCAUUAUCUGUCU, and ACACGGCACUCCUUGGUAU, GE Healthcare Dharmacon. Lafayette CO) using Lipofectamine RNAiMAX Transfection Reagent (ThermoFisher Scientific, Cat# 13778150). After 24 h, media was changed and cells cultured with or without palmitic acid (prepared as a 50 mM stock) at 250-500μM for 14 h. Hepatocytes were then lysed for Western blot analysis or used to assess cytotoxicity utilizing the MTS assay.

For live cell imaging, AML12 cells were treated as above and then stained with propidium iodine and DAPI, according to the manufacturer's instructions.

Figure Legends

Supplemental Figure 1: Liver pathology of C57BL/6 and RIP3-/- mice on high fat diets. Male C57BL/6 and RIP3-deficient mice (RIP3-/- neo) were allowed free access to high-fat diets (HFD) or chow diets for 12 weeks. **(A)** Hemotoxylin and eosin staining of mouse livers. Pathologist scoring of steatosis (% of hepatocytes with macro and/or microvesicular steatosis) was as follows: Wild-type chow 0 $\pm$ 0%, wild-type HFD 36 $\pm$ 15%, RIP3-/- chow 0 $\pm$ 0% and RIP3-/- 75 $\pm$ 15%. **(B)** Frozen liver sections were stained with oil red O. Images are representative of n=4-6 mice per group.

Supplemental Figure 2: Food intake, body weight gain and energy expenditure of C57BL/6 and RIP3-/- on high fat diets. (A) Food intake and body weight of male C57BL/6 and RIP3-deficient mice (Strain containing the neomycin cassette (RIP3-/- (neo)); **(B)** Food intake and body weight gain of male C57BL/6 and RIP3-deficient mice (with the neomycin cassette deleted (RIP3-/- CREΔ)). **(C)** ANCOVA analysis of energy expenditure of C57BL/6 and RIP3-/- (neo) mice between week 10 and week 11 of HFD feeding. Indirect calorimetry was performed on mice fed either CHOW or HFD diet using Columbus Instruments Oxymax/CLAMS system. ANCOVA analysis was used because of the body weight difference between strains on HFD. To account for body size variation on total energy expenditure, group comparisons of energy expenditure (EE) and total body mass (TBM) were made using the linear mixed model, as described in methods. The interactions of EE and TBM were not significant for CHOW diet

(P=0.6029) or HFD (P=0.2246), indicating that there were no differences in energy expenditure between C57BL/6 and RIP3-/- (neo) mice on either CHOW or HFD.

Supplemental Figure 3: Co-localization of TUNEL and F4/80 in livers from C57BL/6 and RIP3-/- mice on high fat diets. Male C57BL/6 and RIP3-deficient mice (RIP3-/- neo) were allowed free access to high-fat diets (HFD) or chow diets for 12 weeks. Paraffin-embedded livers were de-paraffinized followed by TUNEL (Green) and F4/80 staining (Red). Merged images are shown in the right panel. Images were collected with a 40X objective and are representative of at least 5 animals per genotype.

Supplemental Figure 4: siRNA knock-down of RIP3 protein expression in AML12 cells. AML12 cells were transfected with scrambled siRNA or siRNA directed against RIP3. 48 h after transfection, cells were fixed in formalin and RIP3 protein expression detected by immunohistochemistry. Green: RIP3 and Blue: DAPI.

Supplemental Figure 5: Sirius red and collagen 1 in livers of C57BL/6 and RIP3-/- mice on high fat diets. Male C57BL/6 and RIP3-deficient mice (RIP3-/- neo) were allowed free access to high-fat diets (HFD) or chow diets for 12 weeks. **(A)** Liver sections were stained with Sirius red and imaged at 10X. **(B)** Frozen liver sections were used to immuno-detect collagen 1. Images were taken at 20X. Images are representative of 3 areas from 4-6 mice per group.

References

1. Bouret SG, Gorski JN, Patterson CM, Chen S, Levin BE, Simerly RB. Hypothalamic neural projections are permanently disrupted in diet-induced obese rats. Cell Metab 2008;7:179-185.

2. Kaiyala KJ, Morton GJ, Leroux BG, Ogimoto K, Wisse B, Schwartz MW. Identification of body fat mass as a major determinant of metabolic rate in mice. Diabetes 2010;59:1657-1666.

3. Kaiyala KJ, Schwartz MW. Toward a more complete (and less controversial) understanding of energy expenditure and its role in obesity pathogenesis. Diabetes 2011;60:17-23.

4. Mandal P, Roychowdhury S, Park PH, Pratt BT, Roger T, Nagy LE. Adiponectin and heme oxygenase-1 suppress TLR4/MyD88-independent signaling in rat Kupffer cells and in mice after chronic ethanol exposure. J Immunol;185:4928-4937.

Table 1: Fold changes in gene expression relative to C57BL/6 mice on chow diets: RT^2 Profiler^{TM} PCR Array Mouse Insulin Resistance

		Fold Change (comparing to WT Chow)		
		WT HF Diet	**RIPK3 KO Chow Diet**	**RIPK3 KO HF Diet**
Symbol	**Description**	**Fold Change**	**Fold Change**	**Fold Change**
Acaca	Acetyl-Coenzyme A carboxylase alpha	2.0153	1.4938	2.2799
Acacb	Acetyl-Coenzyme A carboxylase beta	1.7303	1.2914	1.9986
Acsl1	Acyl-CoA synthetase long-chain family member 1	0.6246	1.4329	1.0274
Acsl4	Acyl-CoA synthetase long-chain family member 4	0.6648	0.7214	1.5358
Adipoq	Adiponectin, C1Q and collagen domain containing	0.8895	0.8061	0.7679
Adipor1	Adiponectin receptor 1	1.0951	1.2133	1.3651
Adipor2	Adiponectin receptor 2	1.1259	0.9924	1.7041
Akt3	Thymoma viral proto-oncogene 3	1.4251	1.3185	1.6575
Alox5	Arachidonate 5-lipoxygenase	1.2067	1.6806	0.8403
Apoe	Apolipoprotein E	1.3482	1.5357	3.0504
Casp1	Caspase 1	0.8895	1.3745	1.3938
Ccl12	Chemokine (C-C motif) ligand 12	0.8128	3.2692	6.676
Ccr4	Chemokine (C-C motif) receptor 4	0.8895	0.8061	0.7679
Ccr5	Chemokine (C-C motif) receptor 5	0.9272	1.463	2.4777
Ccr6	Chemokine (C-C motif) receptor 6	0.9666	0.5355	0.7786
Cd36	CD36 antigen	1.3765	5.2742	12.9869
Cd3e	CD3 antigen, epsilon polypeptide	0.7584	2.4098	1.2388
Cebpa	CCAAT/enhancer binding protein (C/EBP), alpha	0.9208	0.9454	0.6685
Chuk	Conserved helix-loop-helix ubiquitous kinase	0.8532	1.2561	1.2133
Cnbp	Cellular nucleic acid binding protein	1.2933	1.1321	1.0785
Crlf2	Cytokine receptor-like factor 2	0.6075	0.7732	1.2914
Cs	Citrate synthase	1.6484	1.0784	2.7683
Cxcr3	Chemokine (C-X-C motif) receptor 3	0.9599	0.9259	1.14
Cxcr4	Chemokine (C-X-C motif) receptor 4	0.8957	1.7159	3.9422
Emr1	EGF-like module containing, mucin-like, hormone receptor-like sequence 1	0.8473	1.463	1.4938
Fabp4	Fatty acid binding protein 4, adipocyte	1.2843	2.7874	8.4502
Fasn	Fatty acid synthase	2.2054	1.3094	2.0548
Gys1	Glycogen synthase 1, muscle	0.7584	0.6067	1.5252

Hk2	Hexokinase 2	0.7532	1.3094	3.2921
Ifng	Interferon gamma	1.0651	1.1399	0.9195
Igf1	Insulin-like growth factor 1	0.9938	0.8944	1.0062
Igf1r	Insulin-like growth factor I receptor	1.4856	1.8777	2.4099
Ikbkb	Inhibitor of kappaB kinase beta	0.9938	0.9586	1.1088
Il18r1	Interleukin 18 receptor 1	0.9599	1.3094	0.852
Il1b	Interleukin 1 beta	0.7428	0.9719	3.0293
Il1r1	Interleukin 1 receptor, type I	0.8415	0.9323	2.5651
Il23r	Interleukin 23 receptor	0.8895	0.8061	0.7679
Il6	Interleukin 6	0.8895	0.8061	0.9993
Insr	Insulin receptor	1.3023	1.1479	1.2737
Irs1	Insulin receptor substrate 1	1.6033	0.8944	0.9454
Irs2	Insulin receptor substrate 2	1.0725	0.6731	0.4996
Jak2	Janus kinase 2	1.2067	1.1479	1.5358
Lep	Leptin	0.8895	0.8061	0.7679
Lepr	Leptin receptor	1.3389	1.8907	2.0548
Lipe	Lipase, hormone sensitive	0.629	1.4034	1.2825
Lpl	Lipoprotein lipase	0.7027	3.6526	4.1959
Lta4h	Leukotriene A4 hydrolase	1.0875	1.0345	1.2388
Map2k1	Mitogen-activated protein kinase kinase 1	1.1656	1.0062	1.3746
Mapk3	Mitogen-activated protein kinase 3	1.0505	1.1088	1.071
Mapk9	Mitogen-activated protein kinase 9	1.3482	1.3841	1.3746
Mtor	Mechanistic target of rapamycin (serine/threonine kinase)	1.0951	1.2133	1.5358
Nampt	Nicotinamide phosphoribosyltransferase	1.0432	1.2914	1.8264
Nfkbia	Nuclear factor of kappa light polypeptide gene enhancer in B-cells inhibitor, alpha	0.8772	0.8403	1.2475
Nlrp3	NLR family, pyrin domain containing 3	1.0875	2.0264	2.8264
Olr1	Oxidized low density lipoprotein (lectin-like) receptor 1	0.8895	1.1321	4.4352
Pck1	Phosphoenolpyruvate carboxykinase 1, cytosolic	0.7225	0.3229	0.6281
Pde3b	Phosphodiesterase 3B, cGMP-inhibited	1.3482	0.9069	1.337
Pdk2	Pyruvate dehydrogenase kinase, isoenzyme 2	1.3861	0.8061	1.4231
Pdx1	Pancreatic and duodenal homeobox 1	0.8895	0.8061	0.7679
Pik3ca	Phosphatidylinositol 3-kinase, catalytic, alpha polypeptide	1.3113	1.0417	1.4631
Pik3r1	Phosphatidylinositol 3-kinase, regulatory subunit, polypeptide 1 (p85	1.1656	1.6346	2.0265

	alpha)			
Ppara	Peroxisome proliferator activated receptor alpha	1.3204	1.7159	2.0691
Pparg	Peroxisome proliferator activated receptor gamma	1.0725	2.6371	3.7038
Ppargc1a	Peroxisome proliferative activated receptor, gamma, coactivator 1 alpha	1.4054	1.1883	0.8061
Ptpn1	Protein tyrosine phosphatase, non-receptor type 1	0.54	0.7017	1.7159
Pycard	PYD and CARD domain containing	0.7428	1.2302	1.3841
Rbp4	Retinol binding protein 4, plasma	0.9337	0.9195	0.9006
Rela	V-rel reticuloendotheliosis viral oncogene homolog A (avian)	0.9145	0.8944	1.9439
Retn	Resistin	0.8895	0.8061	0.7679
Rps6kb1	Ribosomal protein S6 kinase, polypeptide 1	0.9467	0.9586	1.0203
Scd1	Stearoyl-Coenzyme A desaturase 1	4.9969	9.9793	13.0773
Serpine1	Serine (or cysteine) peptidase inhibitor, clade E, member 1	1.5922	5.4602	30.2526
Slc27a1	Solute carrier family 27 (fatty acid transporter), member 1	0.8532	1.2388	1.1088
Slc2a4	Solute carrier family 2 (facilitated glucose transporter), member 4	1.683	4.3438	1.4732
Socs3	Suppressor of cytokine signaling 3	2.2362	0.9719	2.4436
Srebf1	Sterol regulatory element binding transcription factor 1	1.1901	3.942	2.8069
Srebf2	Sterol regulatory element binding factor 2	1.2667	0.6593	0.9389
Stat3	Signal transducer and activator of transcription 3	0.7532	0.6547	1.2561
Tlr4	Toll-like receptor 4	1.0505	1.8518	1.669
Tnf	Tumor necrosis factor	0.8895	2.6008	3.315
Tnfrsf1a	Tumor necrosis factor receptor superfamily, member 1a	0.6246	0.8117	1.6234
Tnfrsf1b	Tumor necrosis factor receptor superfamily, member 1b	1.0505	1.0859	1.7888
Ucp1	Uncoupling protein 1 (mitochondrial, proton carrier)	0.8895	0.8061	0.7679
Vldlr	Very low density lipoprotein receptor	6.0672	7.155	12.6318
Control Genes for Normalization:		**Average Ct**	**Average Ct**	**Average Ct**
Actb	Actin, beta	22.57	22.01	21.5
B2m	Beta-2 microglobulin	19.52	19.13	18.92
Gapdh	Glyceraldehyde-3-phosphate	23.37	23.42	22.79

	dehydrogenase			
Gusb	Glucuronidase, beta	28.04	27.64	27.05
Hsp90ab1	Heat shock protein 90 alpha (cytosolic), class B member 1	23.6	23.02	22.61
Experimental Controls:				
MGDC	Mouse Genomic DNA Contamination	35	35	35
RTC	Reverse Transcription Control	23.96	23.75	23.91
RTC	Reverse Transcription Control	23.99	23.75	23.92
RTC	Reverse Transcription Control	24.06	23.67	23.93
PPC	Positive PCR Control	21.26	20.91	21.17
PPC	Positive PCR Control	21.2	20.79	21.04
PPC	Positive PCR Control	21.3	21.79	21.14

Table2: Primer Pairs for Real Time PCR Analysis of Gene Expression

Name	Forward Sequence	Reverse Sequence
18S	ACGGAAGGGCACCACCAGGA	CACCACCACCCACGGAATCG
αSMA	GTCCCAGACATCAGGGAGTAA	TCGGATACTTCAGCGTCAGGA
Col1A1	ATGTTCAGCTTTGTGGACCTC	CAGAAAGCACAGCACTCGC
F4/80	CCCCAGTGTCCTTACAGAGTG	GTGCCCAGAGTGGATGTC T
Fabp4	AAGGTGAAGAGCATCATAACCC	TCACGCCTTTCATAACACATTCC
Fas	AGCGGCCATTTCCATTGCCC	CCATGCCCAGAGGGTGGTTG
IL1beta	ATGGCAACTGTTCCTGAACTCAACT	CAGGACAGGTATAGATTCTTTCCTTT
IL6	TAGTCCTTCCTACCCCAATTTCC	TTGGTCCTTAGCCACTCCTTC
MCP-1	AGGTCCCTGTCATGCTTCTG	TCTGGACCCATTCCTTCTTG
Mgat	TGGTGCCAGTTTGGTTCCAG	TGCTCTGAGGTCGGGTTCA
MMP9	GCGCCACCACAGCCAACTATG	TGGATGCCGTCTATGTCGTCTTTA
MMP13	CTTCTTCTTGTTGAGCTGGACTC	CTGTGGAGGTCACTGTAGACT
Pck1	CGCTGGATGTCGGAAGAG	AGTCTGTCAGTTCAATACCAATC
Ppar-α	AGAGCCCCATCTGTCCTCTC	ACTGGTAGTCTGCAAAACCAAA
Ppar-γ	TCGCTGATGCACTGCCTATG	GAGAGGTCCACAGAGCTGATT
Srebp-1c	AAC GTC ACT TCC AGC TAG AC	CCA CTA AGG TGC CTA CAG AGC
TNFα	CCCTCACACTCAGATCATCTTCT	GCTACGACGTGGGCTACAG

Supplemental Figure 1

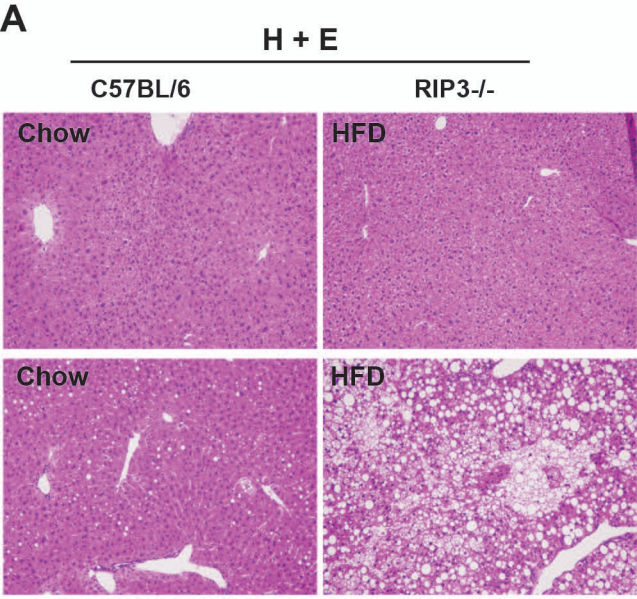

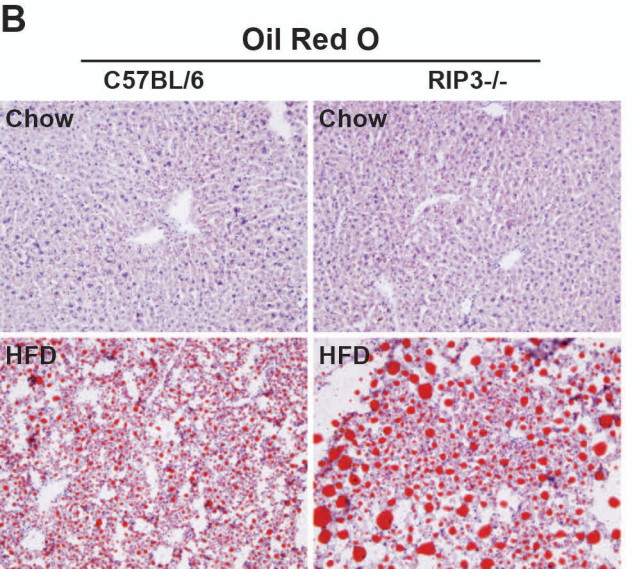

Supplemental Figure 2

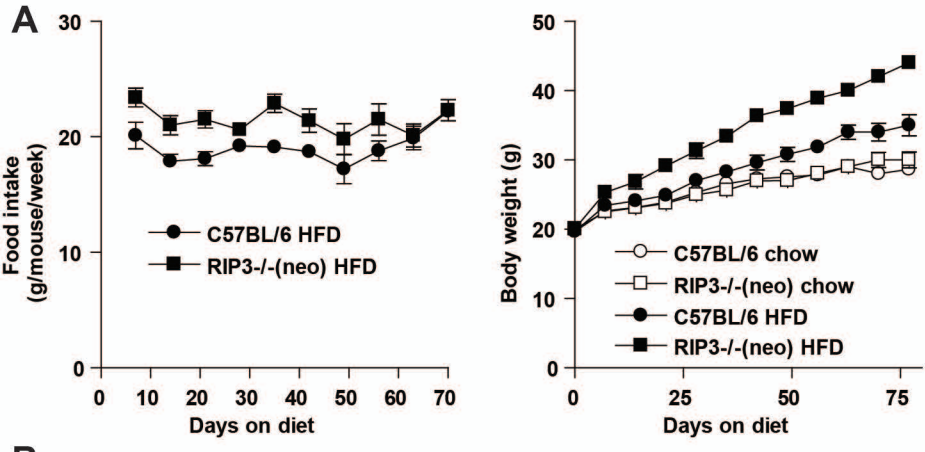

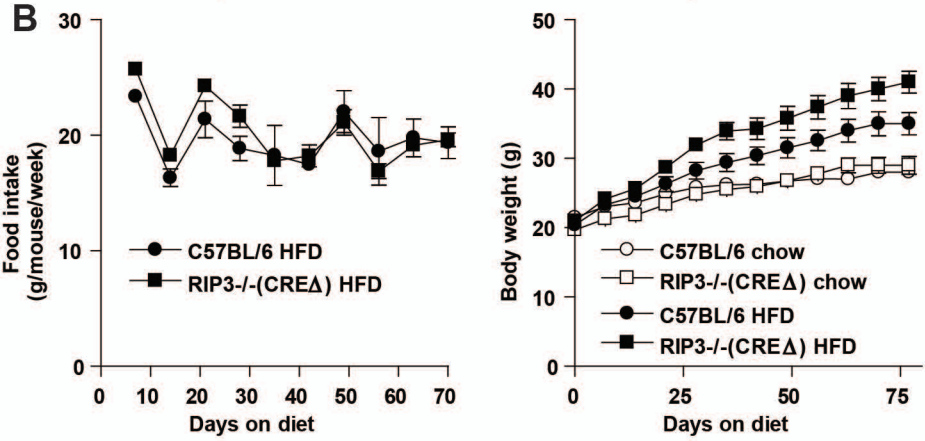

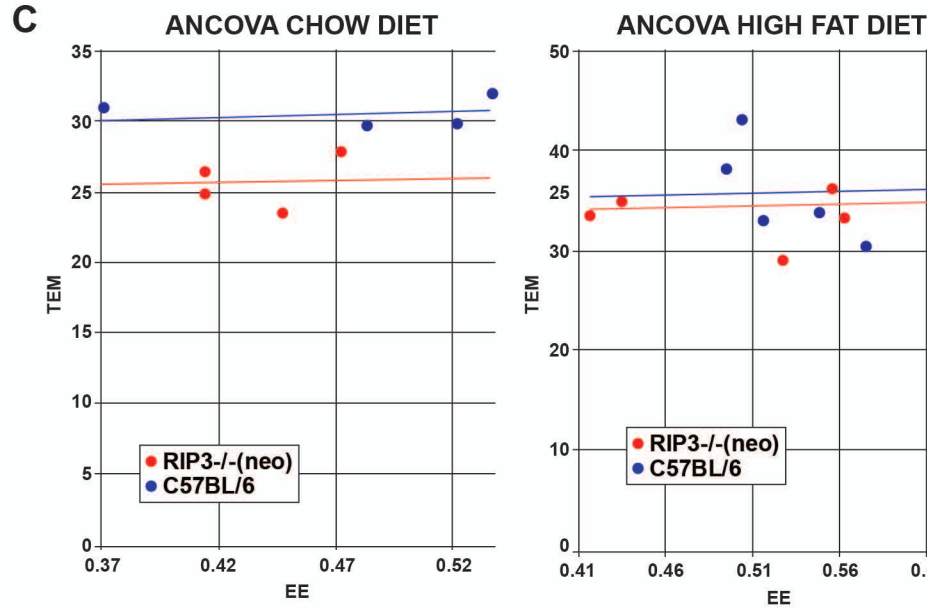

Supplemental Figure 3

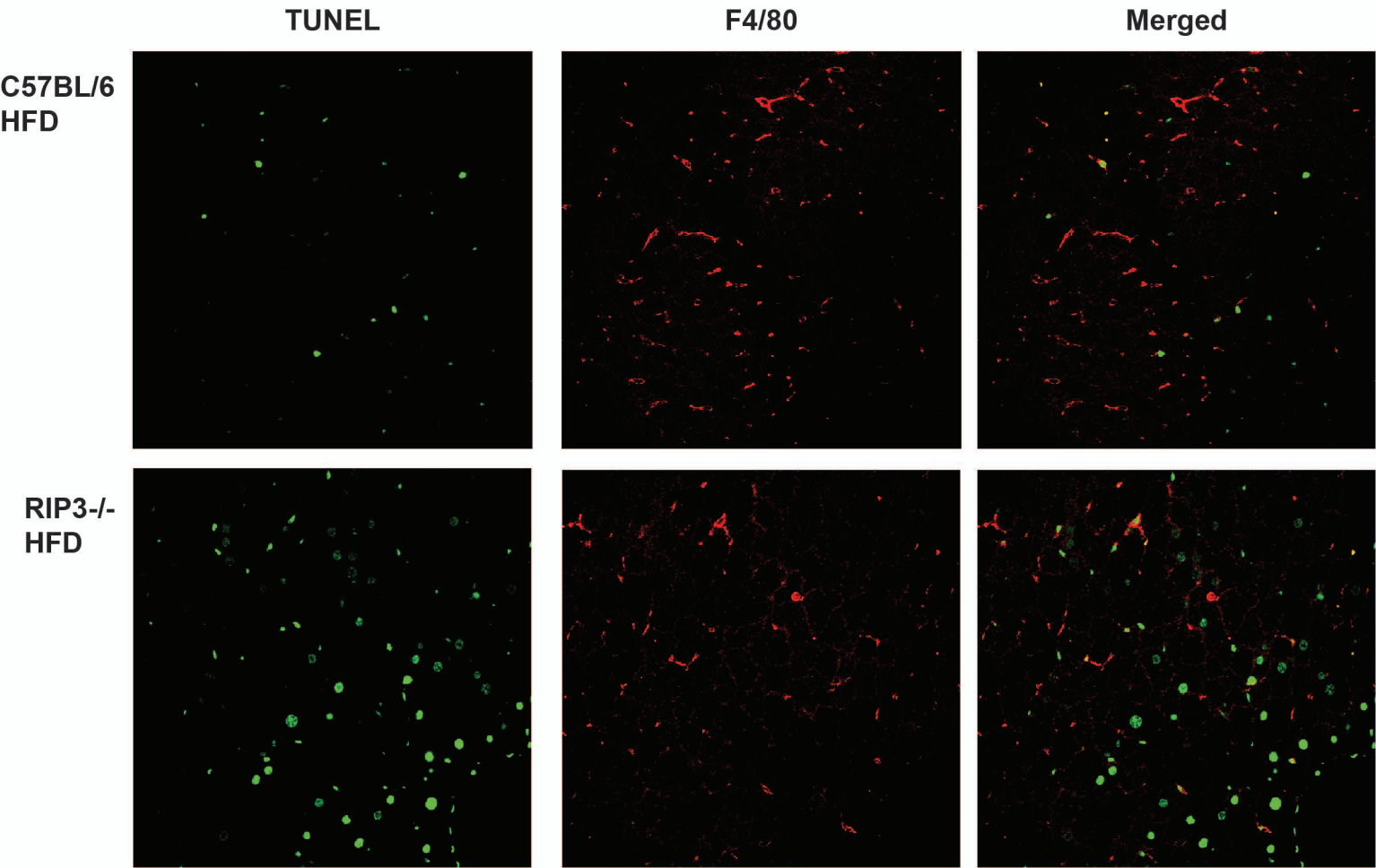

Supplemental Figure 4

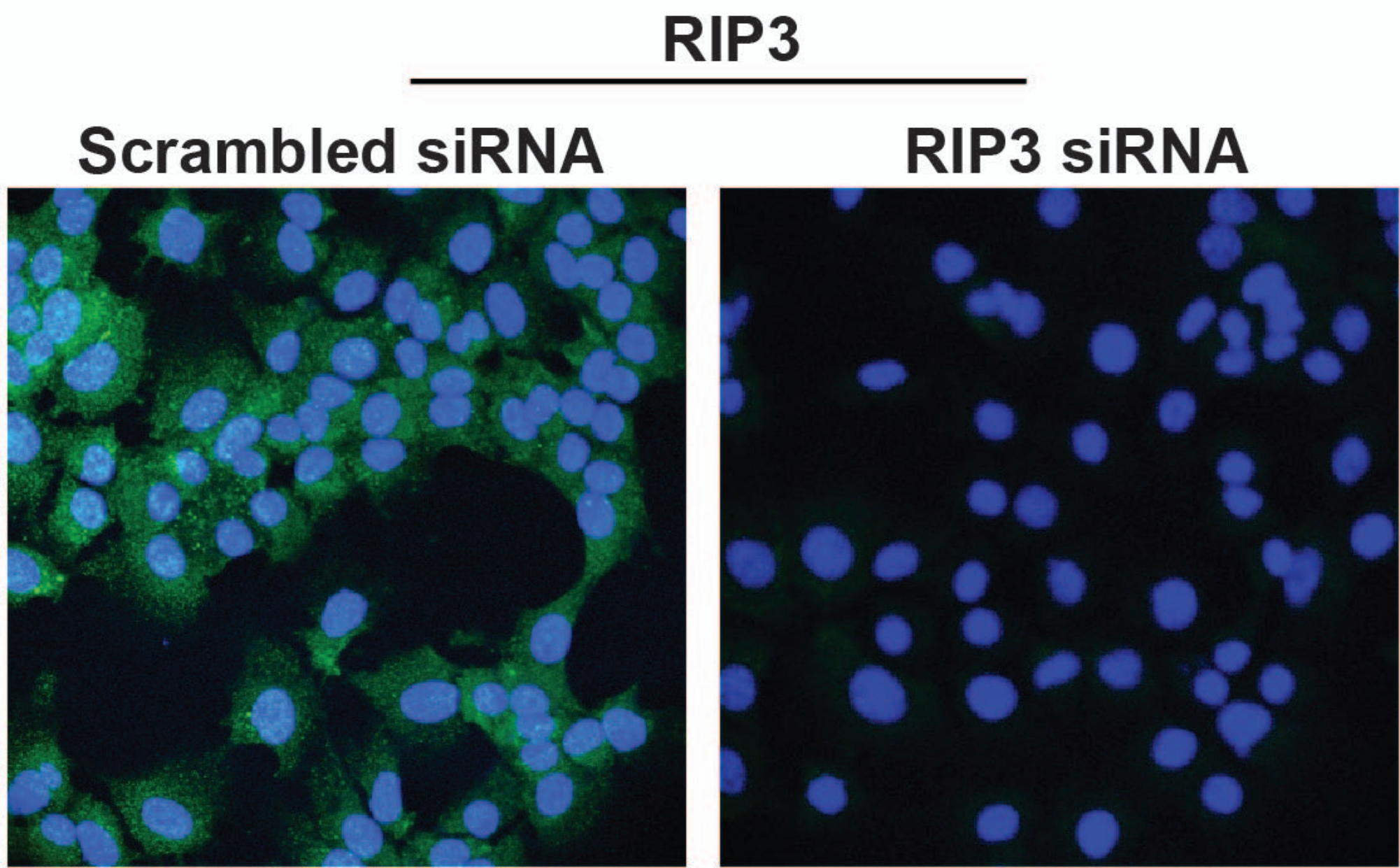

Supplemental Figure 5